Ignition of a Spot Smolder in a Moist Fuel Bed by an Ember

James L Urban[a,*], Jiayun Song[b], Simon Santamaria[c], Carlos Fernandez-Pello[a]

[a] *University of California, Berkeley, Department of Mechanical Engineering, Berkeley, CA, 94720*
[b] *State Key Laboratory of Fire Science, University of Science and Technology of China, Hefei, Anhui 230026, P.R. China*
[c] *The University of Edinburgh, School of Engineering, Edinburgh, UK*

Abstract

Ember or firebrand spotting is an important mechanism by which wildland fires can rapidly spread. This process occurs when embers from a fire upwind land on a fuel downwind. These embers may initiate a fire directly or a smolder fire, which may later transition to flaming in the fuel. The Fuel Moisture Content (FMC) plays an important role in determining whether an ember will ignite the fuel. In this work, the effect of FMC on the smoldering ignition of coastal redwood sawdust by glowing embers of different sizes is studied experimentally. The results show that larger embers are capable of igniting sawdust with a higher FMC. The maximum FMC at which any test resulted in ignition was 40%. The results also showed that for the present experiments, embers smaller than $3.17mm$ in diameter were unable to initiate a smolder in a dry sawdust bed. The ignition boundary is predicted using an energy model which agreed with a multivariate logistic regression of the experimental data using the same functional form.

Keywords: Spot Ignition, Ember Spotting, ignition, wildland urban interface fires, smolder

*Corresponding author
Email address: JLUrban@berkeley.edu (James L Urban)

1. Introduction

Ember or firebrand spotting is a mechanism where small fires are started downwind from burning debris originating from an existing fire. Unlike other fire spread mechanisms, fire spread by ember spotting can be considerably faster if the embers are lofted by the plume of the fire, are subsequently transported by the wind, and then ignite a target fuel if they come into contact with it [1, 2, 3]. Ignition will occur if the ember has sufficient energy to heat, dry and ignite the fuel [4]. Ember spotting can be present in wildland, urban, and Wildland-Urban Interface (WUI) fires. There does not appear to be a consensus on the fraction of structure ignitions caused by embers [5] as it is difficult to determine the ignition source after the fire. However, recent studies attribute the majority of structure ignitions to ember spotting [6, 7].

Recently there have been several large WUI fires across the world. In the state of California alone, there have been several fires over the past two years that are on the top of the California Department of Forestry and Fire Protection's (Cal Fire) lists for top 20 largest (Acres burned) [8], deadliest, and most destructive [9] wildfires. Specifically in the past 2 years, just four of these fires killed 48 people [10], and another group of 4 fires destroyed over 9,000 structures [9] and the fires in the October 2017 fire siege prompted the evacuation of 100,000 people [11]. Dash cam and body cam videos from law enforcement personnel show significant sprays of glowing embers [12] and there are reports of embers igniting spot fires well outside the fire perimeter [13]. There have also been many significant WUI fires which occurred outside of the United States. In 2017, deadly wildfires spread across Portugal burning 500,000 hectares and killing 112 people [14]. There have also been recent significant wildfires in Chile, where 15 people were killed and 2900 homes were destroyed[15]. Recent reports of wildfires in Greece during August of 2018 show a death toll of 98 [16].

The ember spotting process is one example of spot ignition process, the other common one being ignition by hot metal particles. The spot ignition process can be broken down into three sub-processes: (1) the generation of embers or

other hot particles, (2) their coupled transport & thermo-chemical change, and finally (3) the potential target fuel ignition. These sub-processes are illustrated in Fig. 1 [17].

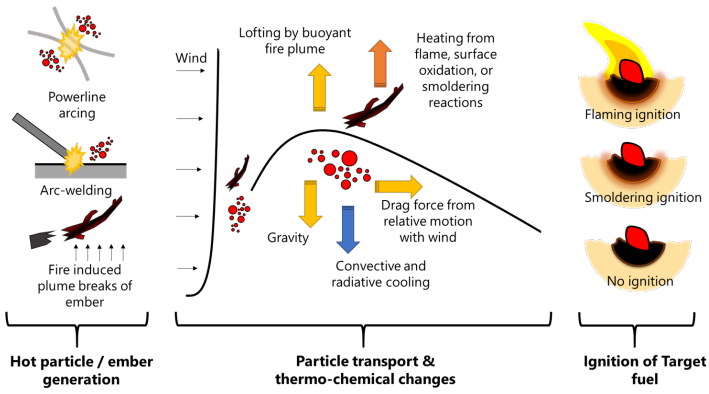

Figure 1: Spotting sub-processes: (1) the generation of embers or other hot particles, (2) their coupled transport and thermo-chemical change, and (3) the potential target fuel ignition.

While the physics governing ember transportation are well understood, the coupled thermo-chemical change undergone by the ember is less understood. Tarifa et al [18, 19, 20] investigated the effect of ember size and degree of mass loss on the burning rate and other parameters useful for understanding the impact of the thermo-chemical change on embers during their transport by the wind. Recent studies have examined the physical processes governing the generation of embers [21, 22] and the embers produced by burning various pieces of vegetation[23] and structures [24, 25, 26]. There have also been studies examining embers and measurements such as ember flux (embers per unit area time) from management-scale wildfire [27].

Recently the impact of the ember burning has also been investigated by researchers comparing the travel distances of burning and non-burning embers [28]. An important but less studied aspect of the transport has been the accumulation of embers near obstacles, which has been only recently studied [29].

There has been a number of ember ignition studies examining the ability of

single or several embers to ignite various fuels by changing parameters of the ember, the fuel, and the ambient conditions [30, 31, 32, 33, 34, 35, 36, 37, 38, 39]. There have also been studies examining the ability of building components to be ignited by ember sprays [40, 41, 42]. Some computational simulations have been made examining the ignition of a fuel by an idealized ember [43, 44].

One very important parameter controlling ignition in spot ignition by embers is the Fuel Moisture Content (FMC). The importance resides in that the ember must evaporate the water in the fuel before it can ignite it, and consequently must have enough energy to first evaporate the water, pyrolyze the fuel and ignite the pyrolyzate [4]. Work has been done investigating the effect of FMC on the net heat released from vegetative fuels [45]. Combined, theoretical and statistical analysis on the effect of FMC on the likelihood of smoldering ignition has been used evaluate the ignition hazard of wildland fuels [46] and utilized results of experiments investigating the ability of simulated embers (matches) to ignite fuels at various FMC levels [47]. However, the theoretical analysis is highly simplified and the ember size is not considered, thus more reliable estimates of ignition probability as a function of FMC are necessary. More recently, the ignition delay time of moist pine needle fuels was explained using a physical correlation for ignition delay time [48]. There have also been studies examining the effect of FMC on fire spread [49, 50] and the FMC has been correlated with the ignition delay time of various fuels [51, 52].

The present study seeks to characterize the ability of single glowing woody embers of varying size to ignite a spot smolder in a natural porous fuel bed at varying levels of FMC. Specifically, the study seeks to find the smolder ignition boundaries (i.e. minimum conditions capable of ignition) for a fuel bed of sawdust of a specified density and FMC when exposed to a glowing wood ember of a given size. The size of the embers are representative of those produced in wildfires and have plausible temperatures and burning conditions for particles produced by these wildfires. The experimental approach is similar to that used by the authors to analyze the smoldering ignition of natural fuel beds by hot metal particles [53], but instead providing ignition boundaries in terms of fuel

FMC and ember size.

2. Experimental Apparatus and Methods

The basic experimental apparatus is a small-scale wind tunnel where a bed of a porous solid fuel is mounted and onto which glowing woody embers are dropped to observe if smolder ignition occurs for a given moisture content of the fuel tested. A simplified schematic and a photograph of the experimental apparatus is shown in Fig. 2. The apparatus is a modification of that used in previous studies [54, 53, 55]. It consists of a bench scale wind tunnel with a test section where the fuel bed is mounted flush with the floor of the tunnel test section. The test section is 55 cm long with a 13 cm by 8 cm cross section with windows on the sides for optical access. The target fuel bed is held in a sample holder such that the fuels free surface is flush to the floor of the test section. The fuel sample holder is 15 cm long, 10 cm wide and 5 cm deep and its leading edge is 15 cm from the inlet of the test section. The top of the wind test section is open so that glowing embers could be dropped onto the fuel.

The woody embers were impaled by a small metal spike 14cm above the fuel bed and ignited by a butane/propane flame for a set amount of time then allowed to freely burn for 10s before having the flame extinguished and removed from the spike so they would fall onto the fuel bed below. To ensure that the embers in the different tests had similar glowing combustion conditions, the time that the embers were exposed to the flame was such that a self-supporting burning of the ember was established, and that the ember could burn to ash completely via glowing combustion if left suspended in the air on the metal spike.

The fuel was imaged from a camera above through the open top of the wind tunnel from which the particles are dropped (Fig. 2). The camera records images of the tests at regular intervals and captures both visible and Infra-Red (IR) light. This allows for visualization of charring of the solid fuel bed, and a qualitative indication of heat losses by IR radiation. In addition to capturing the outcome of the experiment, No Ignition (NI) or Smoldering Ignition (SI)

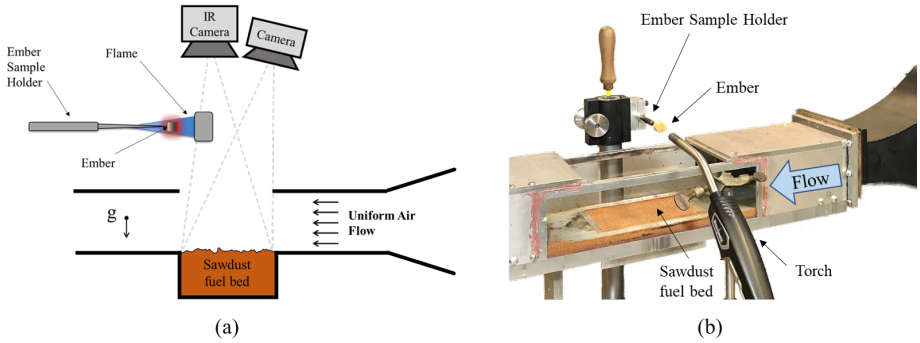

Figure 2: Experimental apparatus, (a) illustration showing camera orientation and (b) photograph of test section, with ember holder and torch for igniting ember.

these pictures provide qualitative data about the temperature of the ember and the presence of solid phase exothermic reactions.

Lab air flows through the wind tunnel with a centerline velocity of 0.5m/s at the leading edge of the fuel for all tests. The air flow velocity is one of many important parameter affecting the ignition process; it affects the rate of oxygen supply to the surface of the fuel and also cools the ember and the smolder developing near the ember. As in other studies with the same apparatus [54, 53, 55], the air velocity in this study was chosen because it produces a uniform flow without disturbing the surface of the fuel. To reduce this irregularity and ensure a uniform cross-flow velocity, embers are only dropped on the leading half of the fuel bed.

The embers in this study were made by cutting wooden dowel rods into cylinders with an aspect ratio of unity. Their diameters ranged in size from 1.6 to 16 mm in diameter. Smaller ember sizes were not considered because the 1.6mm diameter embers failed to ignite fuel bed with a FMC $< 1\%$. The majority of the Fuel Moisture Content (FMC) values tested in this study ranged from 0% to 50% with some up to 70%. The fuel for this study was fine sawdust produced from cutting coastal redwoods *Sequoia sempervirens*. Before use the fuel was stored at different FMC levels in airtight containers which were regularly mixed

to produce uniform fuels. The FMC was measured daily on a dry-mass basis using a sample, at least 3g from each container used. Fuel beds were prepared and used immediately to prevent drying of the fuel before the test. The bulk density of the fuel bed was measured and found to be on average $128 \pm 20\ kg/m^3$ (two standard deviations).

Each experiment resulted in one of two possible outcomes: No Ignition (NI) or Smoldering Ignition (SI). No tests resulted in flaming ignition for the conditions studied and no tests exhibited the transition of smoldering to flaming before they were extinguished. The measurement of larger scale smolder spread was not studied here. Setting a criteria for determining SI compared to NI is more difficult than the analogous case for determining flaming ignition. Here we use criteria used in a previous study examining the ability of hot metal particles to ignite a spot smolder in a natural fuel [53].

For this criteria, SI was determined when the smolder had spread such that it was considerably larger than the ember (1 ember diameter in each direction, measured by eye) and the surface temperature of the fuel surface with an IR camera for evidence of extinction (i.e. temperature well below the boiling point of water). Often at the point of determining the outcome, the ember had been reduced to only ash and thus not driving any potential smolder or retaining any considerable heat. This criteria, was supported by readings from an IR camera, which showed increasing temperatures after a period of cooling. If the smolder had not propagated to the minimum size and cooled to a temperature below $50°C$ after five minutes with no pyrolyzate/smoke production the experiment was deemed a NI event. Tests were not stopped until they reached the criteria of NI or SI. As a final check, a handful of tests were performed where the smoldering front could propagate freely through the entire sample over the course of 1hr and no anomalies were observed.

The experimental data were analyzed using logistic regression to find the ignition boundary. A logistic function, L, shown in Eq. 1 predicts categorical data, such as SI (1) or NI (0), as a probability, $\hat{p}_{SI}$, according to some function, f, such as a function based on the experimental parameters (e.g. ember size and

moisture content) with unknown coefficient. As part of the logistic regression procedure, the unknown coefficients are determined using a maximum likelihood estimate.

$$\hat{p}_{SI} = L(f) = \frac{1}{1 + e^{-f}} \tag{1}$$

Logistic regressions were performed on the experimental data for each ember size, where $f = a + b \cdot FMC$. Later, the experimental data was fit using a function of both ember diameter, d_e and FMC, that shared the functional form of the theoretical model. For details about the use of a maximum likelihood estimate to analyze experimental ignition data, the reader is referred to [56].

3. Results

The direct measurements from each test was the determination of whether either Smoldering Ignition (SI) or No Ignition (NI) occurred after the glowing ember of a given size landed in the fuel bed at a given FMC. In addition, time-lapse images of the IR and visible light were recorded. Images from one experiment showing the smoldering ignition and the initial spread of the smolder reaction along the fuel bed are shown in Fig. 3 for a $4.8mm$ diameter ember. These images were taken with a camera where the there was no infrared filter, so infrared light (shown as the purplish/white glow in Fig. 3) was imaged in addition to the visible light from traditional cameras which have a filter. The purple-white glow in the first image is infrared light imaged by the camera and not representative of what was visually observed by the naked eye, which would instead appear as a red glow. In the second image the ember was mostly ash at this point, but the purplish glow can be seen indicating the presence of infrared light and thus heat release from the smoldering. In the subsequent panels, the glow from the ember is decreasing as the radial charring (smolder) continues to spread along the fuel bed.

An interesting thing to note is that the initial smolder spread is very uniform, almost circular. A previous work found that that the ignition of a spot smolder

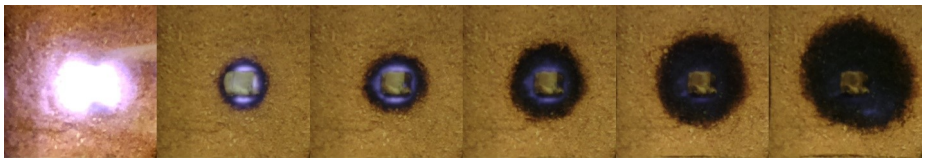

Figure 3: Timelapse images of spot smolder propagation. The purple-white colored light is infra-red light imaged by the camera and not representative of what was visually observed by the human eye. In this test, the outcome could have been recorded at some point after the second to last frame.

by a hot metal particle would often spread in a non-uniform manner [53]. The non-uniform spread in that study was found to be caused by the metal particle because it would first cool as it heated the nearby fuel, igniting an incipient smolder kernel which would then experience heat losses to the metal particle and quench some regions (or all) of the incipient smolder. In the present study, the ember burns for a period of time and leaves behind only a small amount of ash which does not have enough thermal mass to absorb enough heat to interfere with the ignition process in the same way.

From these figures we can also see that the brightness of the glowing decreased substantially over the course of test, indicating that the temperature at the surface was likely highest initially and then decreased. This would not mean however that the smolder was not hot or strong. At the end of tests resulting in SI, the samples quenched and then composted. When removing the spent fuel bed from the holder it became clear that there was substantial, in-depth smolder and that the majority of the smolder reaction front was not at the upper surface of the fuel bed.

The results from the experiments are analyzed using logistic regressions of their observed ignition probability. Several 1-d logistic regression along with a histogram for experimental data of according to ember size are presented in Fig. 4, although tests were also done with embers that were $1.6mm$ and $3.2mm$ in diameter. The $1.6mm$ embers are not plotted because none of the embers ignited a smolder, making logistic regression impossible. The FMC

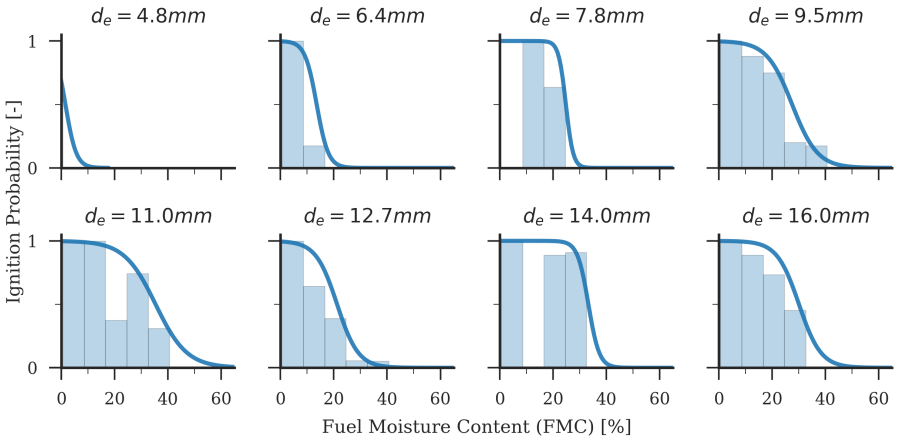

Figure 4: 1-d logistic regressions of smoldering ignition probability as a function of FMC for different ember sizes (ember diameter, d_e) along with histograms of the observed ignition probability.

value where the $3.2mm$ ember would has a 50% ignition probability according to the regression is negative (i.e. non-physical), this does indicate that there are parameters other than FMC that control whether or not ignition happens at this size.

The outcomes of each test are plotted in Fig. 5 with orange X's signifying NI outcomes and blue circles representing SI outcomes. The diameter values of the markers points have been artificially offset about their true value, which are denoted in the horizontal axis tick labels. It can be seen that there are FMC values where both SI and NI events are observed, which makes identifying an ignition boundary (curve separated conditions where ignition was observed from those where it was not observed) not immediately obvious from looking at the raw data by eye. Instead a logistic regression was performed with respect to FMC for each ember size (shown previously in Fig. 4 and the FMCs corresponding to a 50% ignition likelihood and their 95% confidence intervals were calculated. These are plotted over the raw ignition data with a horizontal black line corresponding the 50% ignition boundary and the confidence intervals

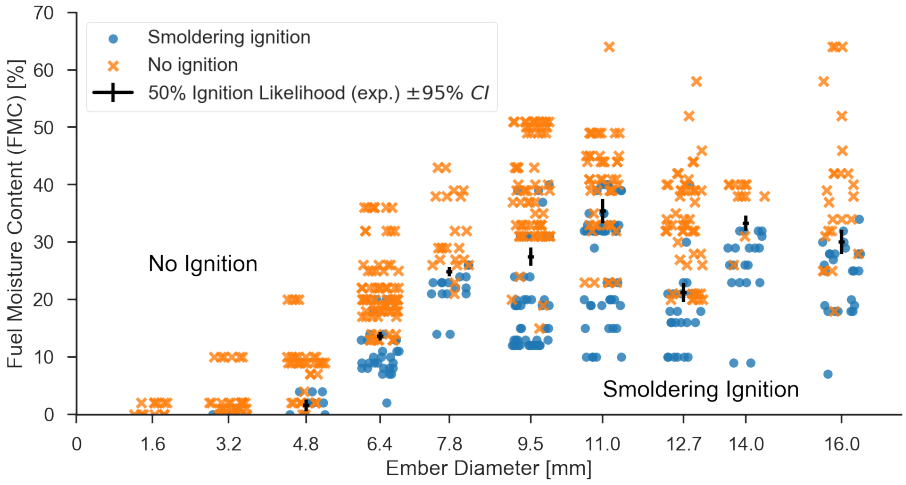

Figure 5: Ignition Results of all tests shown with scatter points with x-values artificially offset to prevent data from obscuring themselves. 50% FMC values calculated from a 1-D logistic regressions for each diameter have been superimposed showing the most likely ignition boundary with 95% confidence intervals.

represented by the endpoints of intersecting vertical lines.

Examining Fig. 5 it can be seem that for a given size ember, increasing the FMC will decrease it's ability to ignite. We can also see that the smallest size, $d_e = 1.6mm$ was not capable of igniting a very dry ($FMC \approx 0$), while an ember where $d_e = 6.4mm$ would because it was capable of igniting a fuel with an $FMC \approx 10\%$ every time. We can also see that for small embers sizes ($d_e < 11mm$), increasing the ember size would allow increase the FMC it is capable of igniting. However for large embers, $d_e > 11mm$, the likelihood for SI to occur is more dependent on changes in the FMC rather than the diameter. One exception is ember size of $12.7mm$ which has somewhat anomalous results compared to the others.

4. Analysis

To understand the observed effect on the fuel bed FMC on the ability of a glowing ember to ignite a smolder in the fuel bed it is helpful to use a simplified

analysis of the heat transfer mechanisms between the ember and the fuel bed. The analysis, which is based on the concept that the glowing (smolder) reactions in both the ember and the fuel bed must release a net positive amount of energy that overcomes the heat losses, helps explain the results of Fig. 5 and provides an analytical expression for the ignition boundary in terms of ember size and fuel bed FMC.

4.1. Energy Model

Given the range of ember sizes in these experiments as well as the effect of FMC, it was hypothesized that SI and NI events can be predicted by an equation comparing the energy released by the ember and the fuel from their smoldering combustion, to the energy needed to evaporate moisture in the fuel and the energy lost to the surroundings. To test this hypothesis, a model was developed to consider the case where the heat released by the smolder reaction just barely overcomes the heat needed to evaporate any moisture and heat losses to the environment. In the model, the system comprises the ember (of diameter d_e) and the nearly fuel bed (a half sphere of diameter $n \cdot d_e$) as shown in the diagram of Fig. 6. The relative size of the surrounding fuel to the ember is left as a general value, n, to generalize the analysis. However, for predicting the ignition boundary it was set to a value of 3, consistent with our experimental criteria for determining SI, when the ignition boundary is plotted in Fig. 7.

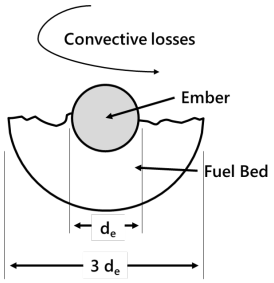

Figure 6: Illustration of ember-fuel bed system.

The model considers the change in the energy of the system between two

states: (1) just as the ember contacts fuel and (2) after the smolder has spread to some diameter $n \cdot d_e$ in the fuel bed. The result is an equation for the net energy of the system, ΔE_{mod}, given by Eq. 2

$$\begin{aligned}\Delta E_{mod} =& V_e \rho_e Q_e - (A_{surf} h_{conv} (T_{sm} - T_\infty) t_e) \\ & - V_F \rho_F \left(c_{p,F}(T_{sm} - T_\infty) + FMC \cdot \Delta h_{vap} + Q_F\right)\end{aligned} \tag{2}$$

where the properties of the ember are: Q_e is the heat released by the ember per unit mass, V_e is the volume, and the density, ρ_e. The time, t_e, is the characteristic time that the ember surface is hot and experiencing significant heat losses and set to 30s based on experimental observations and the time lapse images. The properties of the fuel bed are: Q_F is the heat released per unit mass of fuel, V_F is the volume of the fuel bed, ρ_F is the bulk density of the fuel bed, and $c_{p,F}$ is the specific heat capacity of the fuel. The temperature of smoldering was assumed to be at a representative value T_{sm} and the temperature of the ambient surroundings and the fuel bed before ember contact were both T_∞. The energy required to bring the water in the fuel from T_∞ to saturated steam is Δh_{vap}, which accounts for both the sensible enthalpy and the heat of evaporation. The volumes for the ember and fuel are calculated as a function of ember diameter, treating them as a sphere. The convective heat transfer coefficient for the exposed ember surface can be estimated using the Nusselt number definition, $h_{conv} = Nu \cdot k_{air}/d_e$, and using the Nusselt number correlation for a sphere, found in [57] assuming an average ember diameter for the calculation of the Reynolds number, $10.2mm$, the average diameter for the sizes where the ignition boundary is non-zero ($4.2 - 16mm$). The surface area was assumed to be half that of a sphere, $A_{surf} = \pi d_e^2/2$, assuming that only half the ember is exposed to the surrounding air. The volumes, V_e and V_F are $\pi d_e^3/6$ and $\pi(n \cdot d_e)^3/12$, respectively. The values for the physical parameters used are given in Table 1. The values, Q_e and Q_F are not known because they depend on the percentage of mass consumed by the smolder process, which is unknown in these experiments.

Table 1: Values for parameters used in model

Property	Value	Property	Values
ρ_e (kg/m^3)	283	Q_e (MJ/kg)	0.8
ρ_F (kg/m^3)	128	Q_F (MJ/kg)	1.72
T_{sm} (^oC)	650	T_∞ (^oC)	25
$c_{p,wood}$ $(J/kg-K)$	1380 [57]	Δh_{vap} (kJ/kg)	2552.4
t_e (s)	30		

If the value of ΔE_{mod} is positive then SI is assumed to occur and if it is negative then NI occurs. It should be noted that strictly speaking, negative values of ΔE_{mod} are non-physical which means that an ignition outcome is not possible. The predicted $FMC - d_e$ ignition boundary, the line separating ignition and no ignition results, is given when $\Delta E_{mod} = 0$.

For the purpose of finding the ignition boundary in Fig. 7 it is convenient to create a non-dimensional version of Eq. 2, normalized by the heat released by the ember, $V_e \rho_e Q_e$. The non-dimensional energy change of the system, $\Delta \hat{E}_{mod}(d_e,\ FMC)$, is given in by Eq. 4.

$$\Delta \hat{E}_{mod}(d_e,\ FMC) \equiv \frac{\Delta E_{mod}(d_e,\ FMC)}{V_e \rho_e Q_e} \tag{3}$$

$$= 1 - \frac{Nu \cdot k_{Air}(T_{sm} - T_\infty) \cdot t_e}{2 d_e^2 \rho_e Q_e} - n^3 \frac{\rho_F Q_F}{2 \rho_e Q_e} \left(\frac{c_{p,F}(T_{sm} - T_\infty)}{Q_F} + \frac{FMC \cdot \Delta h_{vap}}{Q_F} - 1 \right) \tag{4}$$

Since we assume ΔE_{mod} (and also $\Delta \hat{E}_{mod}$) is zero valued at the ignition boundary, we can then solve Eq. 4 for the FMC to find the maximum FMC capable of ignition for each ember size, d_e.

$$FMC = \frac{Q_F}{\Delta h_{vap}} - \frac{c_{p,F}(T_{sm} - T_\infty)}{\Delta h_{vap}} + \frac{2 \rho_e Q_e}{n^3 \rho_F \Delta h_{vap}} - \frac{Nu \cdot k_{Air}(T_{sm} - T_\infty) \cdot t_e}{2 d_e^2 n^3 \rho_F \Delta h_{vap}} \tag{5}$$

As noted in the results section, there are two general ignition regions with

respect to the experimental variables (d_e and FMC): first for very large embers ($d_e > 11$) the ignition boundary is very sensitive to the FMC, but insensitive to the ember size. For small embers ($d_e < 11$) ignition is dependent on both FMC and d_e, and there is a minimum size ember capable of igniting a dry fuel bed ($FMC = 0$). To investigate the large ember size behavior with the model we can consider the case of large ember size ($d_e \to \infty$) in Eq. 6.

$$\lim_{d_e \to \infty} FMC = \frac{Q_F - c_{p,F}(T_{sm} - T_\infty)}{\Delta h_{vap}} + \frac{2\rho_e Q_e}{n^3 \rho_F \Delta h_{vap}} \tag{6}$$

and then consider $n \to \infty$, the equation is reduced to, Eq. 7, which gives the maximum FMC level where sustained, adiabatic smoldering is possible. This equation is a form of the energy requirement for smolder propagation with no heat losses which is a function of FMC and not d_e.

$$FMC_{crit} = \lim_{d_e, n \to \infty} FMC = \frac{Q_F - c_{p,F}(T_{sm} - T_\infty)}{\Delta h_{vap}} \tag{7}$$

The heat produced by the smoldering reaction in the fuel, Q_F is an unknown as indicated above, and represents here the net heat released from thermal pyrolysis (endothermic), oxidative pyrolysis (exothermic), and then char oxidation (exothermic) reactions. However, it was estimated by using the experimental value of FMC_{crit} and solving for Q_F. This was done by performing a logistic regression with respect to FMC for the largest four ember sizes which yielded $FMC_{crit} = 30.2\% \pm 1.5\%$ (95% confidence interval) which resulted in a value of $Q_F = 2.17\ MJ/kg$.

In the case of small embers, the ignition boundary is sensitive to the FMC and to the size of the ember. We can examine the limiting case where $FMC \to 0$ in Eq. 4. In this scenario, the ember is on the verge of not having sufficient energy to raise the fuel it is in contact with to a temperature where the smoldering reactions occur. In this case we can calculate a critical ember size, $d_{e,crit}$

given by the equation

$$d_{e,crit} = \sqrt{\left(\frac{Nu \cdot k_{Air}(T_{sm} - T_\infty) \cdot t_e}{\rho_e Q_e}\right)\left[1 + \frac{\rho_F Q_F - n^3 c_{p,F}(T_{sm} - T_\infty)}{\rho_e Q_e}\right]^{-1}} \quad (8)$$

It can be seen that for higher heat losses or less energetic ember or fuel values, $d_{e,crit}$ will increase. This value is important because it provides an estimate of the largest ember size that would be *barely* safe for a given application. In order to obtain a quantitative value of $d_{e,crit}$ it is necessary to know the value of Q_e, which is not well defined because it depends on the amount of ember burned, the composition of the ember and oxygen flow to the glowing combustion reaction zone. Assuming that the ember burns completely a value of $Q_e = 0.8\ MJ/kg$ Can be used which give a value for $d_{e,crit} = 4.7mm$ which agrees approximately with the experimental results

4.2. Statistical Analysis

To further test the model, the experimental data shown in Fig. 5 was fit with a logistic regression where the function, f, from Eq. 1 was a function $\Delta\hat{E}_{reg}(d_e,\ FMC)$, given by Eq. 9. This function has same functional for as the theoretical model, $\Delta\hat{E}_{mod}(d_e,\ FMC)$ in Eq. 4.

$$\Delta\hat{E}_{reg}(d_e,\ FMC) = \ A\ -\ B\ \cdot\ d_e^{-2} -\ C\ \cdot\ FMC \quad (9)$$

The values of the coefficients, A, B, and C are given in Table 2 along with those predicted by the theoretical model. The coefficients are shown in two forms, including one case were the coefficients were rescaled by the values of A. This rescaling is justified when considering the 50% ignition boundary because both the theoretical model and regression model are zero valued at the ignition boundary or 50% ignition contour. Thus multiplying either function when zero-valued by another number (rescaling) would not change the predicted curve. The reason the regression equation has a different scaling is that the scaling relative to the theoretical equation is how the logistic equation resolves the

gradual change in ignition likelihood with respect to FMC and d_e while the theoretical model does not.

Table 2: Coefficients from 2-D regression and theoretical model

	A [-]	B [m^2]	C [-]
2-D Logistic Regression	5.2591	1.1860×10^{-4}	1.5528×10^{1}
Physics-Based model	7.6261	1.6667×10^{-4}	2.1941×10^{1}
2-D Logistic Regression (rescaled)	1	2.2551×10^{-5}	2.9525
Physics-Based model (rescaled)	1	2.1854×10^{-5}	2.8771

The results of the regression and the theoretical model are presented in Fig. 7 with the filled contours indicating the ignition likelihood predicted by the regression, colored according to the colorbar at the right of the figure. The 50% SI probability points from the 1-D logistic regressions for each size (as shown previously in Fig. 5) are superimposed in white for comparison with the multivariate regression. The theoretical model is also included as a black curve. and it agrees well with the multivariate dimensional logistic regression and consequently the ignition data. Overall it is seen that smaller ember size and higher FMC are associated with a lower chance of ignition and larger ember sizes and lower FMC are associated with a higher chance of ignition. The results also display two limiting scenarios. In the case where the FMC is zero, there is a situation where ignition is possible with the smallest ember with diameter, $d_e = 4.7^{+1.2}_{-0.7} mm$ (95% confidence interval). This ember size can also be thought of as the ember size, which would have a 50% chance of igniting for the fuel and conditions considered here.

When the ember is sufficiently large ($> 11.0mm$), the dominant process governing ignition is whether or not the target fuels combustion releases more heat than the energy required to dry the water in the fuel and raise the temperature of the fuel to the temperature at which smoldering reactions will occur. In this area the ignition boundary is dictated only by FMC. It is seen that the 50% ignition boundary for the FMC at which ignition by the larger ember can occur

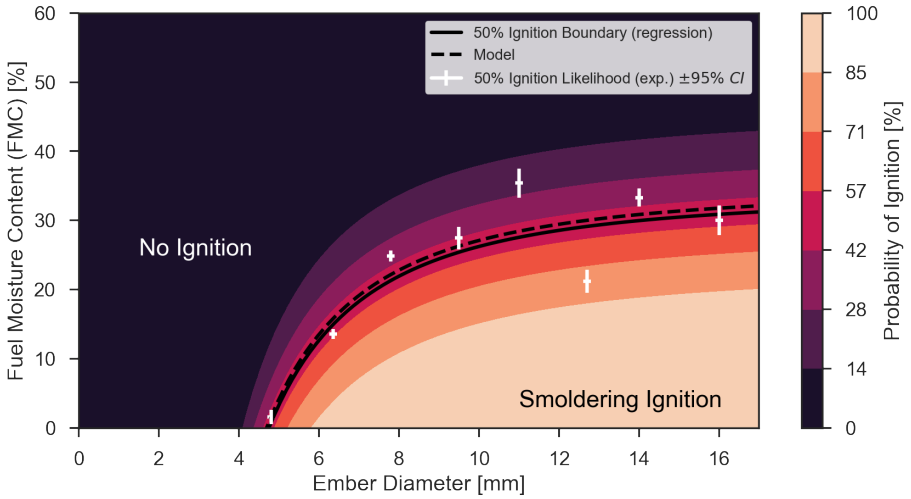

Figure 7: Ignition probability of the sawdust bed at a given FMC by a glowing ember of a given diameter from regression fo data from Fig. 5 with Eq. 9 is shown with the filled contour plot, with colors according to the colorbar on the right.

agrees with the value of 30% predicted by Schroeder [46].

While the 50% ignition probability curve is useful for analyzing the physics of this ignition process, it is a poor metric for the practical consideration of identifying conditions where the chance of ignition is sufficiently low. Instead, for these situations, curves corresponding to a sufficiently low ignition probability, such as the 2.5% (two standard deviation from 50%) would be more useful. These two curves are illustrated in Fig. 8. However, the 2.5 ignition boundary indicates that ignition can occur at FMC of up to 50%, although the probability of ignition would be very low.

It should be noted that in many situations embers are not found alone and often accumulate, creating a different ignition situation [4]. Similar analysis could be performed finding a theory based model for ember accumulations and then analyzed with a similar regression procedure to identify conditions that have a high likelihood of being save and which are demonstrably dangerous.

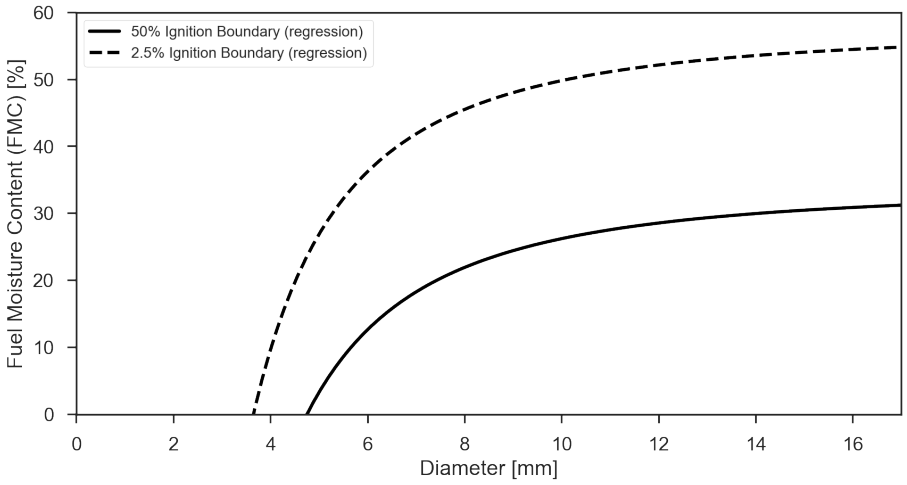

Figure 8: 50% and 2.5% ignition boundaries from logistic regression using Eq. 9.

5. Conclusions

Experiments evaluating the smoldering ignition propensity of glowing embers of various sizes in diameter to ignite a redwood sawdust fuel bed at FMC levels up to 64%. From these data, an ignition boundary based on fuel bed FMC and ember diameter was obtained. As expected, larger diameters are able to ignite fuels with higher FMCs. The maximum FMC at which a test resulted in ignition was 40%. The results also showed that for the present experiments embers smaller than $3.17mm$ in diameter were unable to initiate a smolder in the dry sawdust fuel bed. The results were analyzed using an energy model which predicts the ignition boundary as a function of the ember size and the target FMC. Then a function of the same form with respect to FMC and ember diameter was fit with a multivariate logistic regression and a nearly identical equation was predicted for the ignition boundary. Overall it was seen that smaller ember size and higher FMC were associated with a lower chance of ignition and larger ember sizes and lower FMC were associated with a higher chance of ignition. The results also display two limiting scenarios. In the case where the FMC is zero, there is a situation where ignition is possible with the

smallest ember, $d_e = 4.7^{+1.2}_{-0.7} mm$. This ember size can also be thought of as the largest safe ember size.

When the ember is sufficiently large ($> 11.0mm$), the dominant process governing ignition is whether or not the target fuel's combustion releases more heat than the energy required to dry the water in the fuel and raise the temperature of the fuel to the temperature at which smoldering reactions will occur. In this area the ignition boundary is dictated only by FMC, with FMC $> 30\% \pm 10\%$. The model and regression methodology presented here could be applied to other fuels or other characteristics of embers.

Conflicts of Interest

There is no conflict of interest.

Acknowledgements

This work was supported by a National Defense Science & Engineering Graduate Fellowship, the National Natural Science Foundation of China (Nos. 51625602 and 51476156), the National Key Research and Development Plan (No. 2016YFC0800100), and the Royal Society of Edinburgh. We would also like to thank Adam Huth, Saul Pacheco Elorza, Nicholas Corral, Noeli Paz Soldan, Sivam Paramanathan, Andie Biggs, Kevin Dunnigan, Felix Frank, Jimmy Huang, and Charlotte Dinh who helped with conducting the experiments. The First author would also like to thank Casey Zak who provided useful conversations and suggestions for using a logistic regression.

References

[1] A. C. Fernandez-Pello, C. Lautenberger, D. Rich, C. Zak, J. L. Urban, R. Hadden, S. Scott, S. Fereres, Spot Fire Ignition of Natural Fuel Beds by Hot Metal Particles, Embers, and Sparks, Combustion Science and Technology 187 (1-2) (2014) 269–295. doi:10.1080/00102202.2014.973953.

[2] A. C. Fernandez-Pello, Wildland fire spot ignition by sparks and firebrands, Fire Safety Journal 91 (2017) 2–10. doi:10.1016/j.firesaf.2017.04.040.

[3] R. A. Anthenien, S. D. Tse, A. Carlos Fernandez-Pello, On the trajectories of embers initially elevated or lofted by small scale ground fire plumes in high winds, Fire Safety Journal 41 (5) (2006) 349–363. doi:10.1016/j.firesaf.2006.01.005.

[4] J. L. Urban, A. C. Fernandez-Pello, Ignition, in: S. L. Manzello (Ed.), Encyclopedia of Wildfires and Wildland-Urban Interface (WUI) Fires, Springer, 2018, pp. 1–9.

[5] S. E. Caton, R. S. P. Hakes, D. J. Gorham, A. Zhou, M. J. Gollner, Review of Pathways for Building Fire Spread in the Wildland Urban Interface Part I: Exposure Conditions, Fire Technology (2016) 1–45doi:10.1007/s10694-016-0589-z.

[6] A. Maranghides, W. Mell, Framework for Addressing the National Wildland Urban Interface Fire Problem–Determining Fire and Ember Exposure Zones Using a WUI Hazard Scale, Tech. rep., Nationalist Institute of Standards & Technology (2013). doi:http://dx.doi.org/10.6028/NIST.TN.1748.

[7] W. E. Mell, S. L. Manzello, A. Maranghides, D. Butry, R. G. Rehm, The wildlandurban interface fire problem current approaches and research needs, International Journal of Wildland Fire 19 (2010) 238–251. doi:10.1071/WF07131.

[8] CalFire, Top 20 Largest California Wildfires, Tech. rep., Cal Fire.

[9] CalFire, Top 20 Most Destructive California Wildfires, Tech. rep., Cal Fire (2018).

[10] CalFire, Top 20 Deadliest California Wildfires, Tech. rep., Cal Fire.

[11] CalFire, California Statewide Fire Summary, Tech. rep., Cal Fire (2017).

[12] L. Bonos, A. B. Wang, C. R. Wootson Jr., Santa Rosa, Sonoma, Napa California fires: Death toll rises as winds ease up - (2017).

[13] L. M. Krieger, Wine Country fires: Why are they so deadly, destructive and diffcult to stop? (oct 2017).
URL https://www.mercurynews.com/2017/10/15/california-fires-why-so-deadly-destructive-and-difficult-to-stop/

[14] D. X. Viegas, Wildfires in Portugal, Fire Research 2 (52) (2018) 1. doi:10.4081/fire.2018.52.

[15] P. Reszka, A. Fuentes, The Great Valparaiso Fire and Fire Safety Management in Chile (2015). doi:10.1007/s10694-014-0427-0.

[16] P. Chrysopoulos, East Attica Wild res Death Count Rises to 98 (8 2018).

[17] J. L. Urban, Spot Ignition of Natural Fuels by Hot Metal Particles, Ph.D. thesis, University of California, Berkeley (2017).

[18] C. S. Tarifa, P. P. d. Notario, F. G. Moreno, On the flight paths and lifetimes of burning particles of wood, Symposium (International) on Combustion 10 (1) (1965) 1021–1037. doi:10.1016/S0082-0784(65)80244-2.

[19] C. Tarifa, P. Del Notario, F. Moreno, A. Villa, Transport and combustion of firebrands. U.S. Department of Agriculture Forest Service, Final Report of Grants GF-SP-114 and GF-SP-146, Tech. rep. (1967).

[20] S. Tarifa, P. P. Del Notario, F. G. Moreno, On the Flight Paths and Lifetimes of Burning Particles of Wood, Tenth Symposium (International) on Combustion (1965) 1021–1037.

[21] S. Caton, Laboratory Studies on the Generation of Firebrands From Cylindrical Wooden Dowels (2016).

[22] A. Tohidi, Experimental and Numerical Modeling of Wildfire Spread via Fire Spotting, Ph.D. thesis, Clemson University. doi:10.13140/RG.2.2.13540.58244.

[23] S. L. Manzello, A. Maranghides, W. E. Mell, Firebrand generation from burning vegetation, International Journal of Wildland Fire 16 (4) (2007) 458–462. doi:10.1071/WF06079.

[24] S. Suzuki, S. L. Manzello, Y. Hayashi, The size and mass distribution of firebrands collected from ignited building components exposed to wind, Proceedings of the Combustion Institute 34 (2013) 2479–2485. doi:10.1016/j.proci.2012.06.061.

[25] S. Suzuki, S. L. Manzello, Firebrand production from building components fitted with siding treatments, Fire Safety Journal 80 (2016) 64–70. doi:10.1016/j.firesaf.2016.01.004.

[26] S. Suzuki, A. Brown, S. L. Manzello, J. Suzuki, Y. Hayashi, Firebrands generated from a full-scale structure burning under well-controlled laboratory conditions, Fire Safety Journal 63 (2014) 43–51. doi:10.1016/j.firesaf.2013.11.008.

[27] J. C. Thomas, E. V. Mueller, S. Santamaria, M. Gallagher, M. El Houssami, A. Filkov, K. Clark, N. Skowronski, R. M. Hadden, W. Mell, A. Simeoni, Investigation of firebrand generation from an experimental fire: Development of a reliable data collection methodology, Fire Safety Journal 91 (April) (2017) 864–871. doi:10.1016/j.firesaf.2017.04.002.

[28] J. Song, X. Huang, N. Liu, H. Li, L. Zhang, The Wind Effect on the Transport and Burning of Firebrands, Fire Technology 53 (4) (2017) 1555–1568. doi:10.1007/s10694-017-0647-1.

[29] S. Suzuki, S. L. Manzello, Experimental investigation of firebrand accumulation zones in front of obstacles, Fire Safety Journal 94 (April) (2017) 1–7. doi:10.1016/j.firesaf.2017.08.007.

[30] P. F. M. Ellis, Fuelbed ignition potential and bark morphology explain the notoriety of the eucalypt messmate 'stringybark' for intense spotting, Int. J. Wildl. Fire 20 (7) (2011) 897–907. doi:10.1071/WF10052.

[31] P. F. M. Ellis, Firebrand characteristics of the stringy bark of messmate (Eucalyptus obliqua) investigated using non-tethered samples, Int. J. Wildl. Fire 22 (5) (2013) 642–651. doi:10.1071/WF12141.

[32] P. F. Ellis, The likelihood of ignition of dry-eucalypt forest litter by firebrands, Int. J. Wildl. Fire 24 (2) (2015) 225–235. doi:10.1071/WF14048.

[33] D. X. Viegas, M. Almeida, J. Raposo, R. Oliveira, C. X. Viegas, Ignition of Mediterranean Fuel Beds by Several Types of Firebrands, Fire Technol. 50 (1) (2014) 61–77. doi:10.1007/s10694-012-0267-8.

[34] S. L. Manzello, T. G. Cleary, J. R. Shields, A. Maranghides, W. Mell, J. C. Yang, Experimental investigation of firebrands: Generation and ignition of fuel beds, Fire Safety Journal 43 (2008) 226–233. doi:10.1016/j.firesaf.2006.06.010.

[35] S. L. Manzello, T. G. Cleary, J. R. Shields, J. C. Yang, Ignition of mulch and grasses by firebrands in wildlandurban interface fires, International Journal of Wildland Fire 15 (3) (2006) 427–431. doi:10.1071/WF06031.

[36] S. L. Manzello, S. H. Park, T. G. Cleary, Investigation on the ability of glowing firebrands deposited within crevices to ignite common building materials, Fire Safety Journal 44 (6) (2009) 894–900. doi:10.1016/j.firesaf.2009.05.001.

[37] C. Lautenberger, C. Fernandez-Pello, Generalized pyrolysis model for combustible solids, Fire Safety Journal 44 (6) (2009) 819–839. doi:10.1016/j.firesaf.2009.03.011.

[38] O. Matvienko, D. Kasymov, A. Filkov, O. Daneyko, D. Gorbatov, Simulation of fuel bed ignition by wildland firebrands, International Journal ofWildland Fire (27) (2018) 550561. doi:10.1071/WF17083.

[39] D. P. Kasymov, A. I. Filkov, D. A. Baydarov, O. V. Sharypov, Interaction of smoldering branches and pine bark firebrands with fuel bed at different ambient conditions, in: SPIE, Tomsk, Russia, 2018. doi:10.1117/12.2249083.

[40] S. L. Manzello, S. Suzuki, Y. Hayashi, Exposing siding treatments, walls fitted with eaves, and glazing assemblies to firebrand showers, Fire Safety Journal 50 (2012) 25–34. doi:10.1016/j.firesaf.2012.01.006.

[41] S. L. Manzello, S. Suzuki, Exposing decking assemblies to continuous wind-driven firebrand showers, Fire Safety Science 11 (2014) 1339–1352. doi:10.3801/IAFSS.FSS.11-1339.

[42] S. L. Manzello, S. Suzuki, D. Nii, Full-Scale Experimental Investigation to Quantify Building Component Ignition Vulnerability from Mulch Beds Attacked by Firebrand Showers, Fire Technology 53 (2) (2017) 535–551. doi:10.1007/s10694-015-0537-3.

[43] C. Lautenberger, C. Fernandez-Pello, Modeling ignition of combustible fuel beds by embers and heated particles, Forest fires (2008) 1–13.

[44] C. Lautenberger, A. C. Fernandez-Pello, Spotting ignition of fuel beds by firebrands, in: WIT Transactions on Modelling and Simulation, Vol. 48, WIT Press, 2009, pp. 603–612. doi:10.2495/CMEM090541.

[45] V. Babrauskas, Effective heat of combustion for flaming combustion of conifers, Canadian Journal of Forest Research 36 (3) (2006) 659–663. doi:10.1139/x05-253.

[46] M. J. Schroeder, Ignition Probability, Tech. rep.

[47] W. H. Blackmarr, Moisture content influences ignitability of slash pine litter, Tech. rep., USDA Forest Service (1972).

[48] P. Yin, N. Liu, H. Chen, J. S. Lozano, Y. Shan, New Correlation Between Ignition Time and Moisture Content for Pine Needles Attacked

by Firebrands, Fire Technology 50 (1) (2014) 79–91. doi:10.1007/s10694-012-0272-y.

[49] S. A. Anderson, W. R. Anderson, Ignition and fire spread thresholds in gorse (Ulex europaeus), International Journal of Wildland Fire 19 (5) (2010) 589–598. doi:10.1071/WF09008.

[50] G. M. Davies, C. J. Legg, Fuel Moisture Thresholds in the Flammability of Calluna vulgaris, Fire Technology 47 (2) (2011) 421–436. doi:10.1007/s10694-010-0162-0.

[51] G. Pellizzaro, P. Duce, A. Ventura, P. Zara, Seasonal variations of live moisture content and ignitability in shrubs of the Mediterranean Basin, International Journal of Wildland Fire 16 (5) (2007) 633–641. doi:10.1071/WF05088.

[52] A. P. Dimitrakopoulos, K. K. Papaioannou, Flammability assessment of Mediterranean forest fuels, Fire Technology 37 (2) (2001) 143–152. doi:10.1023/A:1011641601076.

[53] J. L. Urban, C. D. Zak, J. Song, C. Fernandez-Pello, Smoldering spot ignition of natural fuels by a hot metal particle, Proceedings of the Combustion Institute 36 (2) (2016) 3211–3218. doi:10.1016/j.proci.2016.09.014.

[54] J. L. Urban, C. D. Zak, C. Fernandez-Pello, Cellulose spot fire ignition by hot metal particles, Proceedings of the Combustion Institute 35 (3) (2014) 2707–2714. doi:http://dx.doi.org/10.1016/j.proci.2014.05.081.

[55] J. L. Urban, C. Zak, A. Fernandez-Pello, Spot Fire Ignition of Natural Fuels by Hot Aluminum Particles, Fire Technology 54 (2018) 797–808. doi:10.1007/s10694-018-0712-4.

[56] C. Zak, J. Urban, C. Fernandez-pello, Characterizing the Flaming Ignition of Cellulose Fuel Beds by Hot Steel Spheres, Combustion Science and Technology (March 2015) (2014) 37–41. doi:10.1080/00102202.2014.935612.

[57] F. P. Incropera, D. P. DeWitt, T. L. Bergman, A. S. Lavine, Fundamentals of Heat and Mass Transfer, Vol. 6th of Dekker Mechanical Engineering, John Wiley & Sons, 2007.